The Effects of Cloud Model Initialization on Sulfate Chemistry Transport and Wet Deposition over Macedonia

Vlado Spiridonov [a],*, and Mladjen Curic [b]
[a] Institute of Physics, St Cyril and Methodius University, Skopje, Macedonia
[b] Institute of Meteorology, University of Belgrade, Serbia

Abstract

We examine sulfate production and wet deposition over a rural location in Macedonia using a cloud chemistry model and ground-based measurements. The results indicate that using high- resolution meteorological input data from the WRF atmospheric model produces a better simulation and more realistic representation of the cloud-chemistry processes. The method shows a better skill in representation of convective scale processes, the spatial distribution of chemical fields in the cloud environment and thus a more accurate quantitative assessment of sulfate concentration and pH values. Analysis also indicated that scavenging and oxidation are the principal processes affecting sulfate production, participating with 33% and 46%, respectively. Turning off the ice-phase processes leads to overprediction of sulfate aerosol production for about 8 % relative to the base run. This novel method of initialization based on WRF conditions provides a scientific contribution by evaluating simulations of convective clouds in Macedonia against ground-based meteorological and chemical data, as well as by using the model to understand the driving processes affecting sulfate production and wet deposition.

1. Introduction

Convection plays a significant role in vertical transport of atmospheric pollutants, redistribution and wet deposition. Because of this processes the effect of convection is critical to our understanding of air-quality, chemistry-climate and the effect of acidic precipitation on the surface. Many previous studies examined sulfate chemistry processes within cloud using one-dimensional models constraining the physical interpretation of the modelled results [1,2,3], or three-dimensional cloud chemistry model used by Tremblay and Leighton [4] and Niewiadomski [5] but they primarily focused on warm convective clouds. Wang and Chang [6,7]developed and applied a three-dimensional cloud chemistry model to study deep convection and chemical processes, transformations and redistribution of pollutants. The results for a similar research study using different model versions with upgraded microphysics or chemistry parameterizations have been discussed [8 – 14]. Barth et al. [15] examined the redistribution of gases of varied solubility during deep convection, while Yin et al. [16] used a 2-D meteorological model with full microphysics and spectral method of gas scavenging. Ekman et al. [17,18] coupled the cloud-resolving model with an explicit aerosol module to examine aerosol chemistry during deep convection. The evaluation of the results from a number of sensitivity runs implied that accumulation mode aerosols, which play as main cloud condensation nuclei (CCN), are completely removed with heavy precipitation, while nucleation mode aerosols grow fast due to coagulation of aerosols and condensation of S (VI). They also found that the size distribution of aerosols strongly influences their behavior in convective cloud. Stuart and Jacobson [19] investigated the freezing transport mechanism and retention of volatile chemical species in clouds. They argued that cloud model parameterizations which assume that volatiles escape during freezing, tend to over predict partitioning for highly soluble species. In addition, their results imply that for chemical species with low Henry's Law coefficient, freezing conditions have significant impact on retention of chemicals on ice particles. Barth et al. [20] incorporated a simple gas-aqueous chemistry parameterization scheme within Weather Research and Forecasting Model (WRFAqChem) to examine the redistribution of some chemical species by deep convection for the 10 July 1996 STERAO storm. Results indicate significant difference in vertical redistributions of the soluble species considering the freezing transport mechanism (retention and degassing) and also showed some uncertainties in simulation of the influence of deep convection on upper tropospheric composition and chemistry. Wonaschuetz et al. [21] used airborne measurements and parcel model to examine the effects of shallow convection on vertical distribution of aerosol and gases. They emphasized the role of convective transport in altering the vertical distribution of aerosol chemistry and aqueous- phase production of aerosol mass (sulfate and organics). The topography effect on convective cloud evolution and its impact on sulfate transport and redistribution in non-polluted and polluted environment were examined using Advanced Regional Prediction System (ARPS) with coupled aqueous sulfate chemistry sub-model [22]. The results indicate that topography greatly affects the vertical transport of sulfate aerosol. In addition, they found that alternately turning off topography leads to under prediction of Sulphur mass by about

25−30%. Berg et al. [23] incorporated new chemical and microphysical parameterization schemes in WRF-Chem model. This study revealed that these upgraded schemes in WRF-Chem contributed to better forecast of cloud droplet number concentration in a way that is consistent with both high-resolution simulations. This modification also demonstrated ability for a better treatment of cloud aerosol interactions and its life cycle in a realistic manner over regional to synoptic scales. In addition, numerical studies by Barth et al. [24,25] examined the role of deep convection on transport and redistribution of trace gases and aerosols and scavenging by thunderstorms observed over the central U.S. during DC3 field experiments in the central US using for the first time a full set of chemical measurements and ground-based and remote sensing observations. Results show comparable H_2O_2 scavenging efficiency with former studies and also suggest that thermodynamic environment plays a role in the degree of scavenging. As part of this field campaign Bela et al. [26] study reported that high resolution 1 km WRF-Chem with a simple wet scavenging scheme showed ability to simulate storm dynamics and tracer transport quite well and that scavenging efficiency is sensitive to retention fraction of chemical species. However, they suggested that multiphase chemistry cannot be well simulated without detailed aqueous phase chemistry in the model. The initiation of convection depends on many ingredients (e.g. low level convergence, differential heating and strong local forcing environment, moisture transport, wind shear and veering and other factors). The main motivation of the present study is to examine the effect of a new model initialization on deep convective production and deposition of Sulphate. It is achieved using WRF 2.5 km grid forecasts as meteorological input, small temperature perturbation for initiation of convection and fine grid resolution. It makes the model more suitable for the sensitivity simulations show a better skill in resolving of cloud-chemical processes than other cloud chemistry models. Two sets of numerical simulations were done: varying the meteorological initialization, and alternately turning off certain chemical processes participating in sulfate production. In Section 2, we briefly describe the convective cloud model background and sulfate chemistry sub-model, numerical technique and boundary conditions. Numerical experiments, initial conditions and experimental setup are explained in Section 3. Then we focus on evaluation and validation of the results against the observation. Finally, results are discussed and summarized.

2. Model Formulation and Description

2.1. Cloud Model

The cloud model is a 3-D non-hydrostatic, compressible time-dependant, model with dynamic scheme from Klemp and Wilhelmson [27], thermodynamics proposed by Orville and Kopp [28], and bulk microphysical parameterization scheme (see Appendix A) according to Lin et al. [29].

2.2. Sulfate Chemistry Submodel

This model version is coupled with a sulfate chemistry submodel to simulate the chemical and physical processes in convective clouds. Chemical reactions used and corresponding rate coefficients are described in the new article and also listed in Table 1 and 2. Sulfate aerosol chemistry is dominant by aqueous phase reactions on the time scales characterized the convective clouds studied. The chemical fields in the model

and sulfate aerosols expressed in terms of mixing ratios are advected simultaneously with the dynamic and bulk microphysical fields without aerosol bin size used in our model. Only sulfate chemistry is considered in the present version of the model. A more complete set of chemical reactions including CaCO3, MgCO3, Fe3+, Mn2+, methyl hydrogen peroxide and peroxy acetic acid and aqueous phase photochemical reactions i.e. NOx chemistry is definitively desirable. However, the present reactions are sufficient to begin of examination of sulfate chemistry production and wet deposition. Our chemical sub-model uses as basic mathematical framework a set of conventional continuity equations, for each chemical species associated with water category.

Thus, if we denote a concentration of ith pollutant expressed through mixing ratio (q_i) with respect to (water vapor, cloud water and cloud ice); rain; graupel or hail; and snow respectively $q_{i,c}$, $q_{i,r}$, $q_{i,g}$, $q_{i,s}$ the local change of each pollutant separately is given by

$$\frac{\partial q_{i,c}}{\partial t} = -\vec{\vartheta}.\nabla q_{i,c} + \nabla.\mathrm{K}_h\nabla q_{i,c} + SM_{i,c} + SCq$$
(1)

$$\frac{\partial q_{i,r}}{\partial t} = -\vec{\vartheta}.\nabla q_{i,r} + \nabla.\mathrm{K}_m\nabla q_{i,r} + SM_{i,r} + SCq$$
(2)

$$\frac{\partial q_{i,g}}{\partial t} = -\vec{\vartheta}.\nabla q_{i,g} + \nabla.\mathrm{K}_m\nabla q_{i,g} + SM_{i,g} + SCq$$
(3)

$$\frac{\partial q_{i,s}}{\partial t} = -\vec{\vartheta}.\nabla q_{i,s} + \nabla.\mathrm{K}_m\nabla q_{i,s} + SM_{i,s} + SCq$$
(4)

where $\vec{\vartheta}$ represent a velocity vector with components (u, v and w), K_h and K_m are the heat and momentum eddy coefficients. Thus the first two terms on the r.h.s. of the equations (1-4) describe the impact of advection and diffusion, $SM_{i,q}$, $SM_{i,r}$, $SM_{i,g}$, and $SM_{i,s}$ are redistribution terms induced by microphysical conversion processes given by the relation

$$SM_{i,wc} = \frac{q_{i,wc}\,q_m\,(wc \rightarrow i)}{q_{wc}}$$
(5)

where q_m $(wc \rightarrow i)$ is the rate of microphysical transformation derived from the microphysical parameterization scheme. During transformation the water category "wc" will lose mass and the category "i" will gain mass. $q_{i,wc}$ is the mixing ratio of pollutant "i" associated with water category "w_c" and q_{wc} is the mixing ratio of water category. $SC_{i,q}$, $SC_{i,r}$, $SC_{i,g}$, and $SC_{i,s}$ denote chemical transformations terms while $SF_{i,r}$, $SF_{i,g}$, and $SF_{i,s}$ are fallout terms for hydrometeors given by

$$SF_{i,r,g,s} = \frac{1}{\bar{\rho}\rho}\frac{\partial}{\partial \times 3}\left(\bar{\rho}\,U_{r,g,s}\,q_{i,r,g,s}\right)$$
(6)

where $\overline{\rho}$ the initial unperturbed value of air density is, $U_{r,g,s}$ are terminal velocities of rain, graupel or hail and snow, respectively. All chemical fields are expressed in terms of mixing ratios [kg kg^{-1} (air)], while the source terms are written in terms of [kg kg^{-1} (air)]s^{-1}. Seven chemical species groups are included at present time in the model: S (IV), S (VI), H_2O_2, NH_3, N (V), O_3 and CO_2. In dependence of the water categories these species could be found in gaseous, aqueous or solid phase. The absorption of chemical species in the gas phase into the cloud water and rainwater is determined by either Henry's law equilibrium or by mass transfer limitation calculations in order to include the possible non-equilibrium states. Gases, (with an effective Henry's law constant $K_H^* < 10^3$ mol dm^{-3} atm^{-1}) in cloud water and rain are assumed to be in equilibrium with the local gas-phase concentrations. These liquid-phase concentrations of each component (A) are calculated according to Henry's law; i.e.

$$\lfloor A \rfloor = K_H \, p_A \tag{7}$$

where [A]A/L H_2O or M is in units of mole, K_H is the Henry's law coefficient (M atm^{-1}) and p_A is the partial pressure of the species [A] in atm unit. All equilibrium constants and oxidation reactions are temperature dependent according to van't-Hoff equation.

$$K_T = K_{T0}\exp\left\lfloor -\Delta H / R(1/T - 1/T_0)\right\rfloor \tag{8}$$

where ΔH is the increase of enthalpy induced by chemical reactions K_{T0} is the equilibrium constant at a standard $T_0=298$ K and R is the universal gas constant. However, a chemical species may not attain equilibrium on the timescales of the cloud model because of slow mass transfer between phases. In that case a fully kinetic calculation of gas dissolution into the cloud droplets and raindrops is included in the model. The rate of mass transfers between gas species "i "and drops with radius **r** and number of concentrations N_r (per mole air), could be expressed by the following relation according to Yin et al. [16]

$$\frac{dq_{d,i,r}}{dt} = \frac{3\eta D_{g,i} N_{Sh,i}}{RT\overline{r}^2}\left[V_r N_r P_i - \right. \tag{9}$$

Here $\overline{r}$ is the mass mean radius of cloud drops and raindrops. We made some assumptions in regard to definition on radius of drops. Since the cloud water is assumed to be monodisperse, for the mean mass radius of cloud drops is taken as 10μm. The mean radius for the raindrops is 2λ-1 where λ is the slope intercept parameter in the raindrops size distribution where ρ is the air density, q_{cw} the cloud water mixing ratio and M_w is the mean mass of cloud drops.

$C_{d,i,r}$ is the molar mixing ratio with respect to air of gas species **i**, inside drops with radius r, K_H^* the effective Henry's Law constant of species **i**, R the universal gas constant, T the temperature; $D_{g,i}$ the diffusivity of gases **i** in air, V_r the volume of drops with radius r, P_i the partial pressure of gas species **i** in the environment, $N_{Sh,I}$ the mass ventilation coefficient (Sherwood number) which depends of solubility of species, and ŋ a factor which is a function of the Knudsen-number K_n and sticking coefficient λ_i of gas species **i** on spherical drops. The present research describes in detail sulfate chemistry as it was done in study by Taylor [3]. Sulfate production and

subsequent deposition through precipitationm are considered by the following processes: chemical reactions (gas conversion + oxidation), scavenging of aerosol particles and transfer of the atmospheric pollutants by the microphysical transitions. A schematic of the aqueous phase sulfate processes is shown in Fig. 1. and listed in Appendix B. The term for nucleation scavenging (PS3) simply models the primary activation of cloud condensation nuclei (CCN). The nucleation efficiency indicates that 80-100 % of the total aerosol mass is activated and incorporated into cloud drops when there is condensation. According to Taylor [3] this process is parameterized using

$$\left\{ \begin{array}{ll} \dfrac{\varepsilon SO_4^{-2} \, qSO_4^{-2}}{\delta t}, & \delta q_c \geq 0 \\ 0, & \delta q_c \leq 0 \end{array} \right. \tag{10}$$

where $\varepsilon SO_4^{-2} = 0.55$ is fractional nucleation efficiency, δq_c is the condensation of cloud drops during the current time step. The condensation rate for cloud water is denoted by $\delta q_c / \delta t$ and is calculated as the difference between total cloud water at grid point prior to the temperature adjustment required to bring the water fields and energy into equilibrium after advection, and after the temperature adjustment step. In addition, cloud and rain drops contain dissolved ammonium sulfate $(NH_4)_2SO_4$ which is not created or destroyed in the chemical reactions. The only transitions of NH_4^+ aerosol are scavenging and those following the microphysical transfer. The source terms for H_2O_2, SO_2 and O_3 which schematic is illustrated in Fig.2 and also listed in Appendix C. The equilibrium [H$^+$] concentration in cloud water and rainwater is calculated under assumption that hydrogen ion concentration [HSO$_3^-$] is the dominant form of S(IV) and as the results that S(IV) mole fraction of [SO$_3^{-2}$] is less than 3% for the pH range found in this clouds 3 ≤ pH ≤ 5.5, only [HSO$_3^-$] is included in the charge balance equation. Thus, the calculation of the cloud water pH and rainwater pH is based on the equilibrium hydrogen ion concentration for [H$^+$], which is given by the simple charge balance equation [3]:

$$[H^+] = 0.5 \left| 2[SO_4^{2-}] - [NH_4^+] + ((2[SO_4^{2-}] - [NH_4^+]) \right. \tag{11}$$

As we already mentioned only sulfate chemistry is considered in the present version of the model. A more complete set of chemical reactions and aqueous phase photochemical reactions i.e. NO$_x$ chemistry is definitely desirable to reveal the true condition. The chemical reactions expressed through equilibrium reactions and dissociation and the corresponding coefficients are listed in Tab.1, while S (IV) oxidation reactions and associated coefficients are shown in Tab.2. More information regarding the cloud physics, sulfate chemistry parameterization, initial and boundary conditions and model initialization could be found in [30,12,13,31].

Table 1 Equilibrium reactions and rate coefficients

No	Reaction	K_{298} (M or M atm^{-1})	$-H_{298}/R(K)$	Reference	
1.	$SO_2(g) \Leftrightarrow SO_2(aq)$	1.2	3135.	Hoffmann and Calvert	(1985)
2.	$SO_2(aq) \Leftrightarrow HSO_3^- + H^+$	1.3×10^{-2}	2000.	Hoffmann and Calvert	(1985)
3.	$HSO_3^- \Leftrightarrow SO_3^{-2} + H^+$	6.3×10^{-8}	1495.	Hoffmann and Calvert	(1985)
4.	$O_3(g) \Leftrightarrow O_3(aq)$	1.13×10^{-2}	2300.	Pandis and Seinfield	(1989)
5.	$H_2O_2(g) \Leftrightarrow H_2O_2$	7.1×10^4	6800	Martin and Damaschen	(1981)
6.	$NH_3(g) \Leftrightarrow NH_4OH(aq)$	75	3400	Pandis and Seinfield	(1989)
7.	$HNO_3(g) \Leftrightarrow HNO_3(aq)$	2.1×10^5	8700.	Schwartz and White	(1981)
8.	$CO_2(g) \Leftrightarrow CO_2(aq)$	3.4×10^{-2}	3420.	Pandis and Seinfield	(1989)

Table 2 S(IV) oxidations and the corresponding coefficients

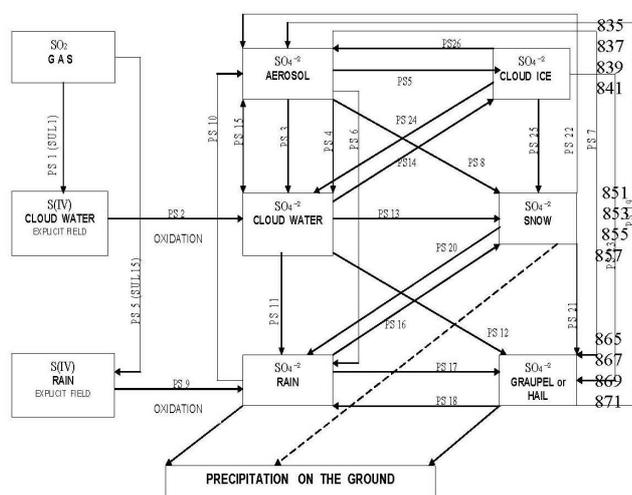| No	Reaction	K_{298} (M^{n}s^{-1})	$-\Delta H_{298}/R(K)$	Reference	
9.	$S(IV) + O_3 \rightarrow S(IV) + O_2$	3.7×10^3	5530	Hoffmann and Calvert	(1985)
10.	$S(IV) + H_2O_2 \rightarrow S(IV) + H_2O$	7.45×10^7	4751	Hoffmann and Calvert	(1985)

Figure 1: Schematic of SO_4^{-2} reactions and microphysical transitions
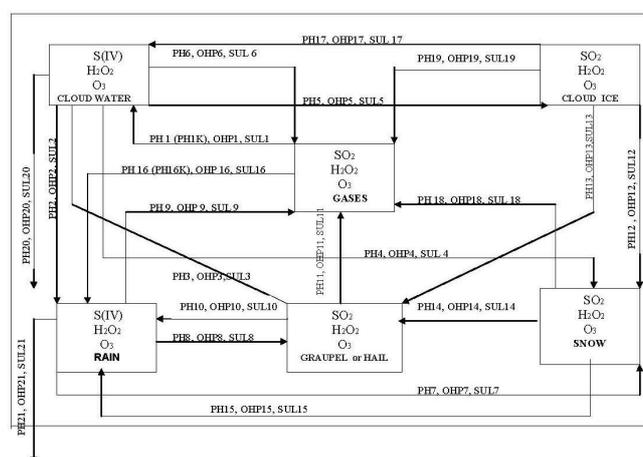

Figure 2: Schematic of H_2O_2, SO_2 and O_3 reactions and microphysical transitions

3. Observational Analysis and Model Setup

3.1 In Situ Data

Convection plays an important role in sulfate vertical transport and redistribution and may act as an important source of sulfate in the air. Such local-scale air pollution episodes which affect the local chemical composition, air and water quality and in some situation exceeding international standards were observed and measured in Macedonia during March-April 2000. A significant amount of sulphate aerosol concentration was measured in Macedonia on 3 April 2000, with a local maximum value of sulphate volume concentration of 6.69 (mg/l) at Lazaropole station located in the rural representative area. The precipitation samples are collected every 24 hours with a Wet Only Sampler ARS 1510. The laboratory analysis has been performed using a standard method of anion elements. The initial results show some visible yellowish aerosol particles partially dissolved in precipitation. The increase of content of all chemical species (e.g. anions, cations and heavy metals), significantly changed the qualitative-quantitative features and acidity. Sensitivity experiments indicate that the maximum sulfate volume concentration of 7.2 (mg/l) occurred

on 3 April 2000 and therefore it was chosen for the following sensitivity test.

3.2 WRF Model Configuration

Weather Research Forecast Non-Hydrostatic Mesoscale Model WRF-NMM v.3.6 [32 – 34] has been used in the present research. The physical parameterization package of the model includes: planetary boundary layer (PBL), microphysics (MPS), the surface processes, turbulent mixing, convection, radiation and diffusion. The PBL parameterization is based on Mellor–Yamada–Janjic (MYJ) scheme, which employs 1.5 order turbulence closure model, according to Mellor and Yamada (1982) and Janjic [35,36,32]. The parameterization of the convective processes is based on Betts-Miller-Janjic scheme, Janjic [36]. The Noah land-surface scheme is based on Chen and Dudhia [37].

The model microphysics is based on WRF Single-Moment 6-Class (241 WSM6) microphysics Hong et al. [38]. WRF forecasts for each selected day have been performed using NCEP FNL (Final) operational global analysis and forecast data on 0.25 by 0.25-degree grids prepared operationally every six hours, interpolated to a WRF single model domain. The model configurations adopted over three model domains are

displayed on Fig. 3. The entire grid system has 38 vertical layers with a terrain following hybrid sigma coordinate, and the model top is located at 50 hPa. All sensitivity WRF 10, 5 and 2.5 km runs have the consistent initialization time at 06 UTC, and cover the same forecast period of 24 h. The first 6 hours of 249 the simulation represent a spinup period.
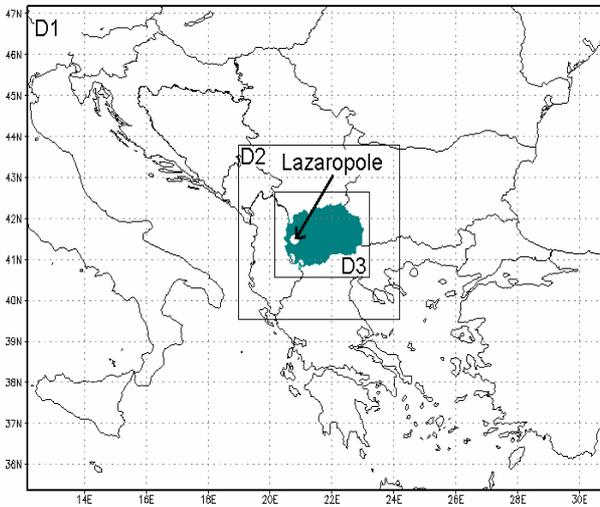

Figure 3: The model selected domains. The outer box is domain 1 (10 km). The inner boxes denote the domain 2 (5 km), domain 3 (2.5 km), respectively.

3.3 Cloud Chemistry Model Initialization and Initial Fields

The environment encompassing Lazaropole station was assumed to be homogeneous, so the single meteorological and chemical profiles were used for initialization of cloud chemistry model simulations. As this particular event is strongly sensitive to the detail mesoscale initialization, our basic approach is to employ four different initialization approaches for this experimental setup. The vertical stratification of the atmosphere (potential temperature, specific moisture and the horizontal velocity components) creates the initial meteorological input (Fig.4) for running the model. An atmospheric profile identifies several important instability features that might be responsible for the initiation and evolution of this convective event. The WRF profiles indicate decrease in potential temperature profile at 3 km height, moisture deficit at the near surface layer (2.5 km), wind veering and enhanced wind shear in PBL layer. Initial meteorological parameters provided from the upper air sounding show relatively lower moisture content, continuous increase of the potential temperature with height, low wind shear in the PBL and enhanced upper level zonal wind compared to WRF profiles. The chemical input data are separately taken and vertically interpolated in the central point of the model domain. The initial chemical profiles are taken from the measurement data set for Lazaropole for 3 April 2000. Fig.5 shows the vertical profiles of sulfate aerosol, Sulphur dioxide, ammonia in airgap $\times$ kg^{-1} (air), hydrogen peroxide and ozone (ppbv). The initiation of convection is performed using thermal bubble with a minimal temperature perturbation in its center. This model setup with fine horizontal grid resolution of 500 m and 250 m vertically gives some advantages in better representation and treatment of the convective scale and chemistry processes which are on a subscale model domain in respect to the numerical scheme. The sensitivity runs have been performed using a three-dimensional version of the model with very fine spatial resolution of 0.5 km x 0.5 x 0.25 km. Since the model equations are compressible, a time-splitting procedure is applied to achieve numerical efficiency and

stability. Thus sound-wave terms are solved separately using a smaller time step$\Delta t = 1$ s, while all other equations are treated with a larger time step $\Delta t = 5$s which is appropriate for the time scales of physical interest. The cloud model domain covers atmospheric volume with dimensions 81 x 81 x 16 km^3 or 161x161x60 grid points. The initial impulse for convection is the ellipsoidal thermal bubble positioned 15 km to the left in the central portion of the cloud model domain, at height of 2.0 km. The radial dimensions of the bubble are x* =15 km, y* = 15 km and z* = 3.5 km, respectively. The temperature and velocity perturbations respectively have maximum values in the bubble's centre and exponentially decrease towards zero at the bubble's boundaries. The cloud-chemistry sensitivity tests have been performed for a period of 2 hours at the most intense phase of cloud evolution. Traditionally, for cloud model initiation and running we require initial meteorological parameters from upper air sounding and initialization using thermal bubble with maximum temperature and vertical velocity perturbation in its centre. The upper air soundings are usually located on a certain distance from the area of interest. The present approach proposes using initial data from WRF 2.5 km forecast model in given location and time. It produces a more detail information about the local meteorological environment. The cloud chemistry model is also initialized with thermal bubble but the initiation of convection does not depend too much from the modeller as the minimum temperature perturbation is required. In general, the present approach gives some advantages in cloud model initialization and initiation of convection, better treatment of the cloud-chemistry processes which are on sub-scale in respect to the model and lower central processing unit CPU time needed for integration under fine resolution computing mode.
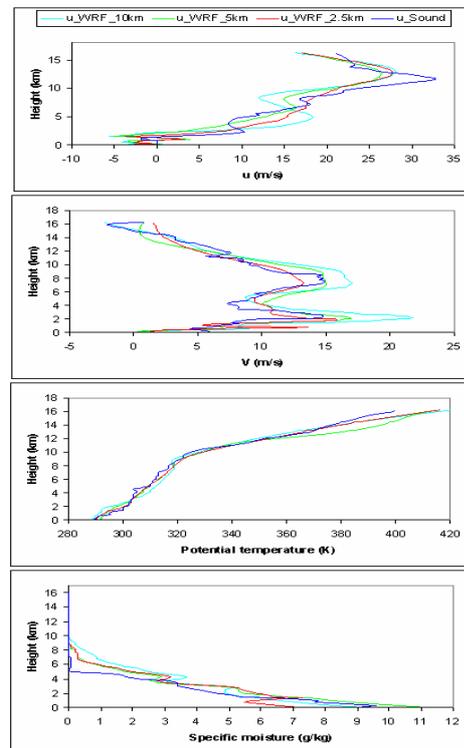

Figure 4: Vertical profiles of u and v-velocity components, potential temperature and specific humidity for Lazaropole case on 3 April 2000.
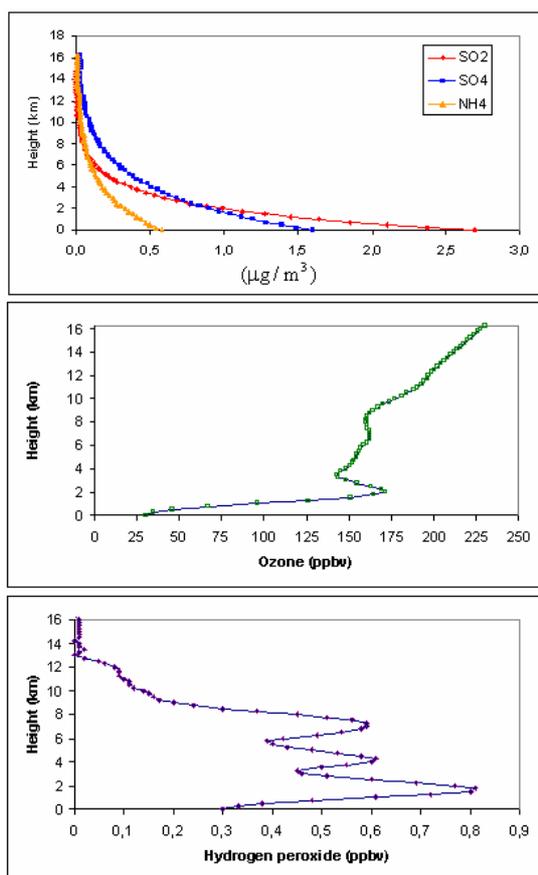
Figure 5: Initial vertical profiles of (a) sulfate aerosol, sulfur dioxide, ammonia aerosol, hydrogen peroxide and ozone for Lazaropole on 3 April 2000

4.0 Model Results

The cloud-chemistry model initialized with WRF derived input is running separately for each selected date during a two months period. In addition, 3 April has been selected as peak rainfall and sulfate aerosol wet deposition was observed. Two types of sensitivity simulations are conducted: varying the meteorological initialization, and alternately turning off certain chemical processes.

4.1 Sulfate Chemistry Simulations under Different Meteorological Initialization

Cloud-chemistry model running with WRF derived input is a good choice in case when upper air sounding is missing, or its location is on a certain distance from the area of interest (as our case). Thus the available measurements of vertical stratification of the atmosphere are not really representative and therefore interpolation procedure should be applied in order to provide reliable meteorological information. The first model run is specified by meteorological parameters obtained from an observed upper air sounding. Other numerical simulations have been initialized from WRF model forecasts with different spatial and temporal resolutions. In both cases the initial meteorological fields are homogenous and vertically interpolated in the central point of the cloud model domain. The sensitivity experiments have been performed employing WRF initialization and derived initial fields with 10, 5 and 2.5 km grid resolution. Fig. 6 depicts the spatial distributions of sulfate volume concentration in 25 min, at the most intense phase of cloud evolution, using a different model initialization. It is apparent that simulation with the upper air sounding

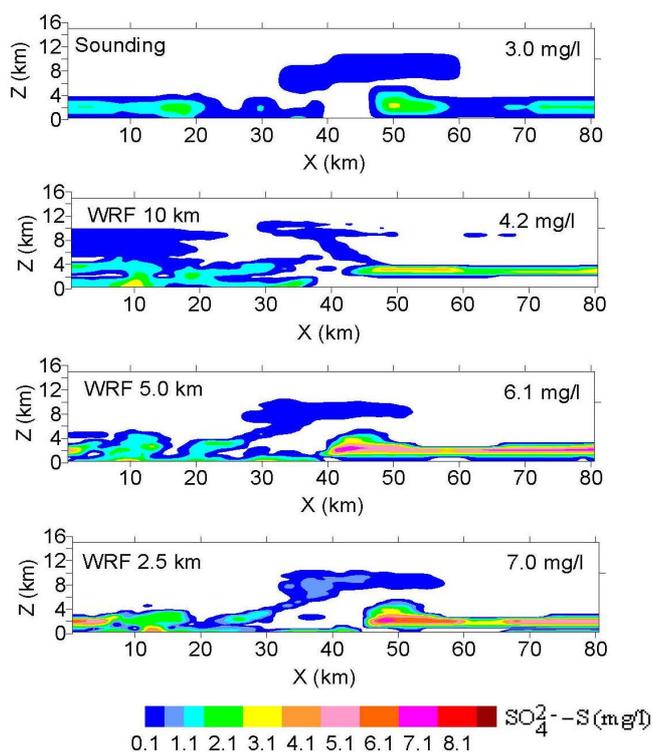initialization shows a more uniform distribution of sulfate aerosol mass.

Figure 6: Spatial distributions of sulfate volume concentration in 25 min of the simulation time using a different model initialization.

The sulfate concentration averaged over the simulation time indicates about two times lower value relative to measured volume concentration at the meteorological station Lazaropole. The similar result with slightly higher sulfate concentration of 4.2 mg/l is obtained using initialization with WRF 10 km and applying cumulus parameterization. The cloud model simulation with initial meteorological parameters derived from WRF 5 and 2.5 km forecasts and explicit treatment of convection shows a more detail representation of the sulfate aerosol transport and redistribution and thus a better quantitative estimation of the sulfate volume concentration of 7.0 mg/l which is similar to that obtained from laboratory measurement. That is mainly due to better initial meteorological input and finer spatial and temporal resolution of cloud model that is capable to resolve the convective scale processes in more detail. These factors are dominant for cloud-chemical processes interaction, and the modification of sulfate concentration which influences on sulfate budget and acidity of precipitation. We continue with the examination of the spatial distributions of the sulfate aerosol in condensate phase from 5 to 60 min of the simulation time as depicted in Fig. 7. The dashed curve delineates the cloud boundary, while the solid curves represent isopleths of sulfate expressed as volume concentration. The numerical simulation has shown initial convection evolved from a stratified cloud environment. We note a near cloud base convergence detected in the vortex area embedded between forward flank updraft and rear flank downdraft region. The rapid vertical transport of sulfate in the cloud developing stage is due to updraft and the mass transfer by nucleation scavenging of the sulfate particle matter. The nucleation process of sulfate aerosol is important as it represents the primary activation of cloud condensation nuclei (CCN). The nucleation efficiency indicates that 80-100 % of

the total aerosol mass is activated and incorporated into cloud drops when there is condensation. This process occurs at a cloud base and the numerical simulation indicates an increase concentration at the initial stage of cloud evolution at the cloud base.

Subsequently sulfate parcel with relatively lower concentration is advected and diffused by the turbulent flow toward the upper portion of the cloud. Early formation of rainfall contributed in acceleration of the microphysical transfer process among water categories and sulphate mass conversions between other chemical species participating in sulfate production and wet deposition. After this the updrafts are not sufficient to maintain sulphate mass at the cloud base, and washout by rain gradually reduced cloud dissolved sulphate. From 40 min of the simulation time, enhanced zonal circulation at the upper levels move the sulfate mass in the central part of the model domain-contributing to more uniform distribution of sulfate. It is seen that the rain loaded sulfate in small fractions reaches the ground leading to wet deposition. Soon after that when the cloud enters dissipation stage a new cloud movement and activity is detected at the inner portion of the cloud model domain. The spatial distribution of H_2O_2, O_3, NH_4^+, SO_2 and SO_4^{2-} of chemical species participating in sulfate production and wet deposition during most intense stage of cloud evolution is shown in Fig. 8. In parallel, as the illustration we present time evolution of vertical profiles of the microphysical fields, wind structure and updrafts and downdrafts. We note a more rapid vertical transport of ozone, hydrogen peroxide and sulfate maximum concentration and a maximum mixing ratio located near the central part of the simulated cloud. Fig. 9 displays the vertical profiles of microphysical fields, wind structure and updrafts and downdrafts as demonstration of the importance of physical processes upon sulfate chemistry. The formation of rain gradually reduces the mass of dissolved sulphate (Fig. 9a). After that, formation of anvil becomes apparent. A new cell is initiated at the outflow boundary on the down shear side of the convective cloud (see Fig. 9b), between updraft and downdraft regions in the lower part of the atmosphere (Fig. 9c). It is accompanied by the strong vertical gradient at cloud base as the result of sulfate mass transfer by nucleation scavenging. Here the maximum concentration of 365 sulfate aerosol mass is apparent.
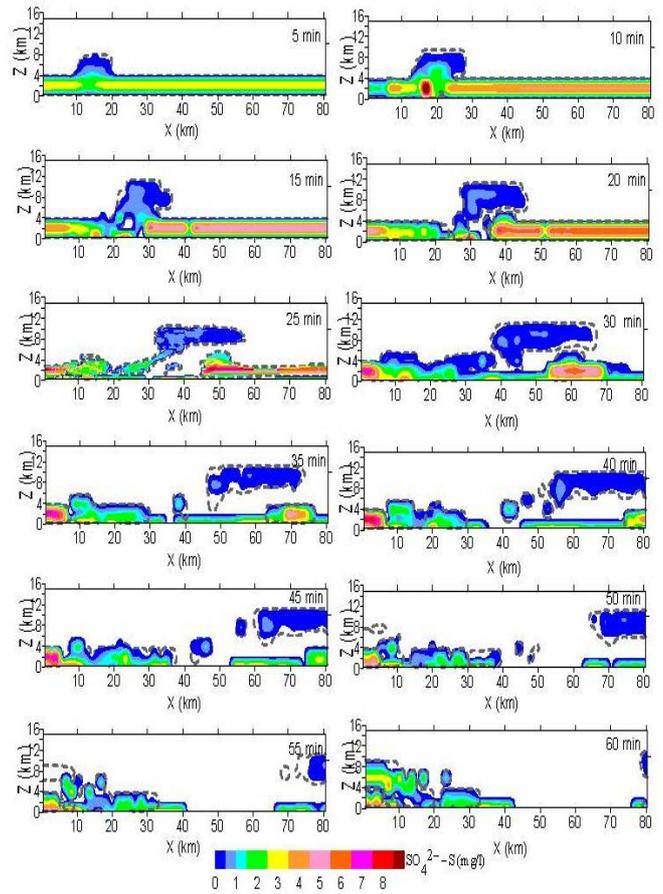

Figure 7: Spatial distribution of the sulfate volume concentration (mg/l) from 5 to 60 min of the simulation time at 5 min time intervals of Lazaropole case using 2.5 km WRF initialization.
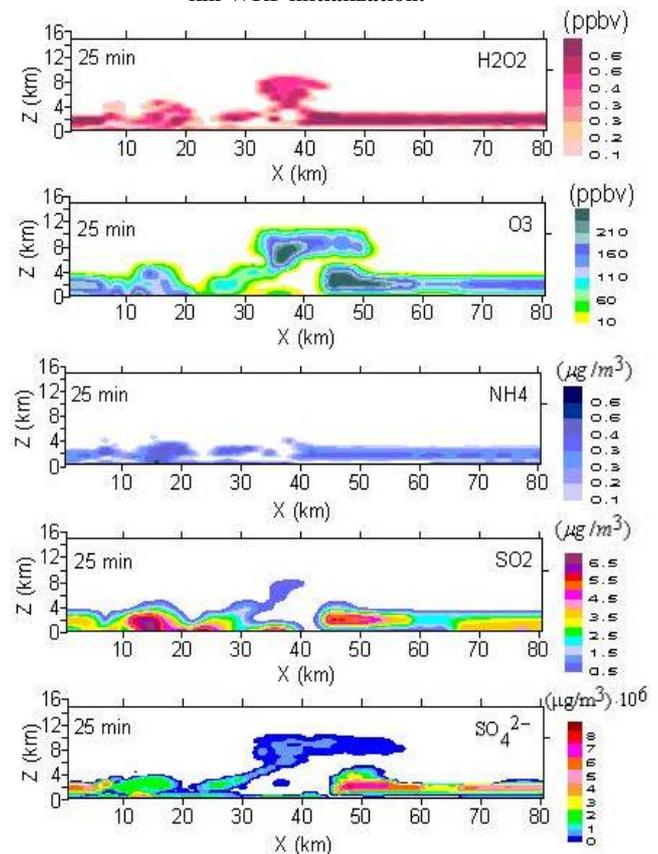
Figure 8: Spatial distribution of chemical species in condensate phase participating in sulfate production and wet deposition
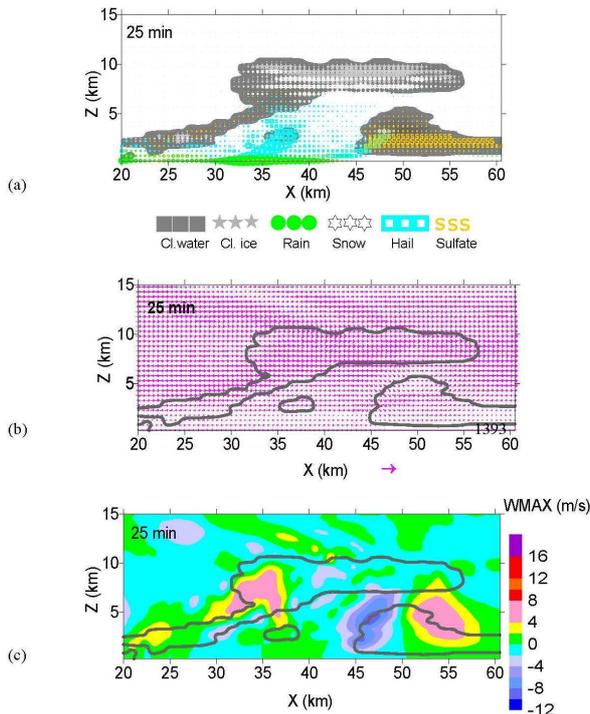

Figure 9: a) Spatial distribution of microphysical fields and sulfate in 25 min of the simulation time; b) Vertical profile of the wind field; c) Updrafts and downdrafts in simulated cloud.

4.2 The Relative Importance of Various Processes Participating in Sulfate Chemistry

Our second task was to examine the relative importance of scavenging, oxidation and ice-phase processes in the model, which influences the sulfate budget and acidity. In addition, a fully explicit calculation of gas dissolution in cloud water has been applied and compared with the base run. Fig. 10 exhibits the vertical profiles of sulfate aerosol, alternately turning off certain chemical processes which influence on sulfate production and wet removal. The first panel shows the base run with a Henry's law equilibrium. It is obvious that the run using mass transfer limitation calculation (bottom panel) shows a closer value (6.5 mg/l) with that measured at the meteorological station Lazaropole on 3 April 2000 (6.690 mg/l).The difference is apparent for more soluble gases as hydrogen peroxide. The assumption of Henry's law equilibrium in this case leads to about 4.6 % higher value of SO_4^{2-} (mg/l) compared to the kinetic gas uptake method. The scavenging is found to be very important process for the redistribution of chemical species. Many past studies have been focused on examination of scavenging processes by convective clouds using scavenging coefficient as the first order removal according to Giorgi and Chameides [39], wet deposition fluxes Easter and Hales [40], a two-component mixture method proposed by Cohan et al. [41] or the combination of the last two approaches Barth et al. [15]. Yin at al. [16] proposed spectral method of gas scavenging while Crutzen and Lawrence [42] introduced portioning between interstitial and condensate phases for soluble species to parameterize precipitation washout. In Spiridonov and Curic [13] the efficiency of scavenging processes were explicitly calculated

and determined from the model generated microphysical and chemical fields and results showed that by ignoring scavenging in such convective clouds can cause decrease of concentration inside cloud and in the near-cloud environment. Bae et al. [43] more recently incorporated a new scheme in Community Multiscale Air Quality (CMAQ) model to examine the below-cloud scavenging processes on aerosol budget over East Asia. Their new below-cloud scavenging method differs from other previous approaches as they 391 use the collection efficiency mechanisms, terminal velocity of raindrops, raindrop-size and particle-size distributions. Their results indicated that this novel approach shows a more efficient rate of wet removal and better agreement with observation, in particular for convective rainfall.

In the present study, we examine both: in-cloud (nucleation aerosol and scavenging by cloud droplets via Brownian diffusion) and dynamic impact scavenging by falling hydrometeor (below-cloud scavenging). Based on the results in-cloud and below-cloud scavenging accounted for 25% and 35%, respectively. Fig. 10 b shows the integrated aerosol scavenging (when in-cloud and subcloud scavenging are alternately excluded) which tends to underestimate the amount of sulfate mass (5 mg/l) or about 30% relative to the base run.

Of particular interest for aqueous sulfate chemistry are the reactions through which S (IV) is oxidized to S (VI) by H_2O_2 and O_3 in the liquid phase. Elimination of oxidation terms leaves scavenging of SO_4^{2-} aerosol as the only remaining pathway for the SO_4^{2-} found in precipitation. In our case the exclusion of oxidation processes leads to lower sulfate aerosol concentration of 3.8 mg/l (46%) than the base run. As we have noted SO_4^{2-} is produced by oxidation of S (IV) to SO_4^{2-} in cloud droplets and rainwater by SO_2 and O_3. Ignoring the ice processes means that we are assuming the same chemical evolution as in liquid medium or ice fields is treated as liquid medium for chemistry. In such case H_2O_2 is dominant everywhere while SO_2 oxidation is limited by the amount and the short transit time in a lower portion of the cloud couples with oxidation temperature and pH factor. This difference becomes more evident in cloud mature stage and heavy precipitation period. In such case when the ice processes are neglected may lead to an overestimate of sulfate aerosol concentration through SO_2 oxidation in instances of intermediate H_2O_2 concentration.

Ignoring the ice-phase processes, considering numerical simulation with 414 initial data from WRF 2.5 km forecast, may lead to overestimate sulfate volume concentration by about 8%, relative to the base run. Vertical distribution cloud water pH at the most intense phase of evolution using a different model initialization is displayed in Fig. 11. The main characteristics of the diagram is the strong vertical gradient and similar pattern distributions of cloud water during development phase of cloud evolution. The difference between the vertical sections inside the cloud is more evident in run with 2.5 km initialization as the result of early dissolution of pollutant near the cloud base relative to other runs. The rainwater pH (see Fig. 12) shows a strong gradient at the near surface layer with spatial displacement of the shapes in all runs derived from WRF forecasts with an averaged pH value decreased to 4.5 in 2.5 km run. On the other hand, the simulation using upper air sounding as model initialization and initial data input-the rainwater pH develops into an irregular shape (not shown) followed by a weakening as the results of early washout and partial evaporation.
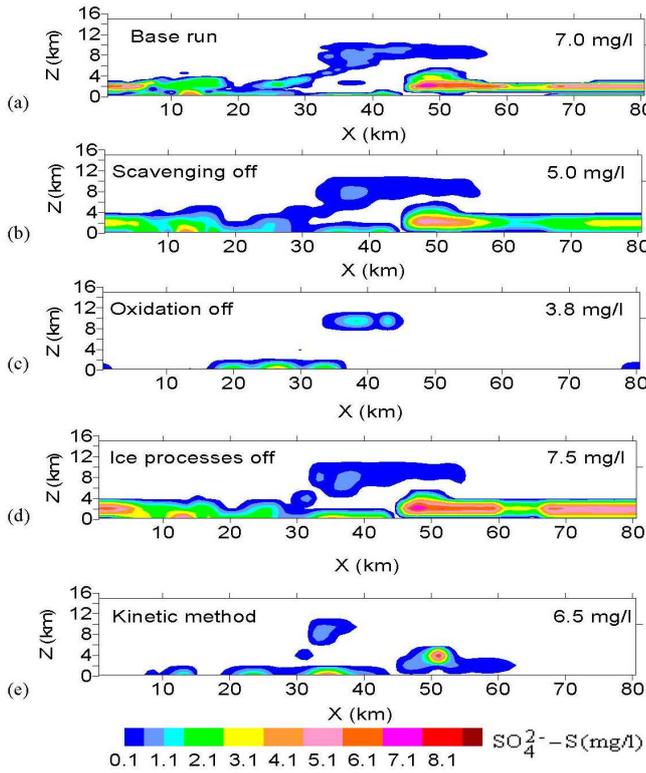
16

Figure 10. Spatial distribution of the sulfate mixing ratio (mg/l) in 25 min of the simulation time (developing stage) alternately turning off certain chemical processes. The panels from top to the bottom display: the base run simulation, turning off scavenging off, oxidation off; ignoring ice processes; and simulation with kinetic gas uptake, respectively.

Figure 11: Vertical profile of cloud water pH during developing phase of cloud evolution using a different model initialization
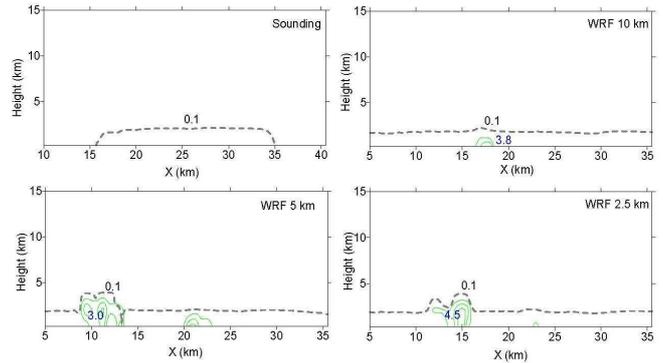

Figure 12: Same as Figure11 but for rainwater pH

4.3 Comparison with observations and laboratory measurements

Results obtained using this coupled cloud chemistry model have also been compared with available in situ physical and chemical measurements provided from a special ground sampling meteorological station Lazaropole located in a remote rural representative area. Figs. 13 shows this comparison between the sulfate volume concentration, pH value and sulfate wet deposition with simulated parameters during March-April 2000. In general, there is a relatively good agreement between the measured and simulated results during the entire analyzed period. The difference between the results becomes more evident when cloud chemistry model is initialized with upper air sounding data and WRF 10 km grid resolution. It is apparent that the maximum amount of rainfall, pH, volume concentration of SO_4^{2-} and wet deposition of Sulphur is measured on 3 April 2000. Here, 2.5 km run shows quite reasonable values of sulfate aerosol concentration and pH.
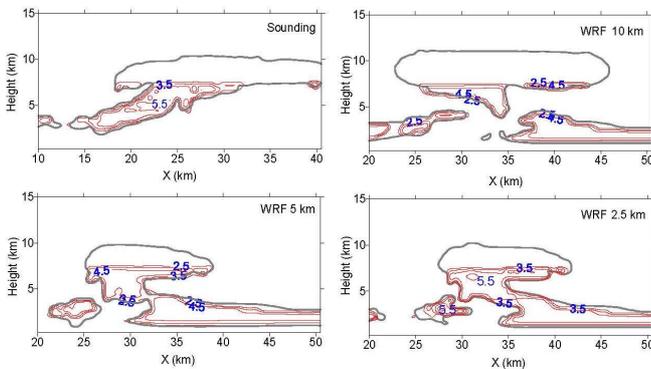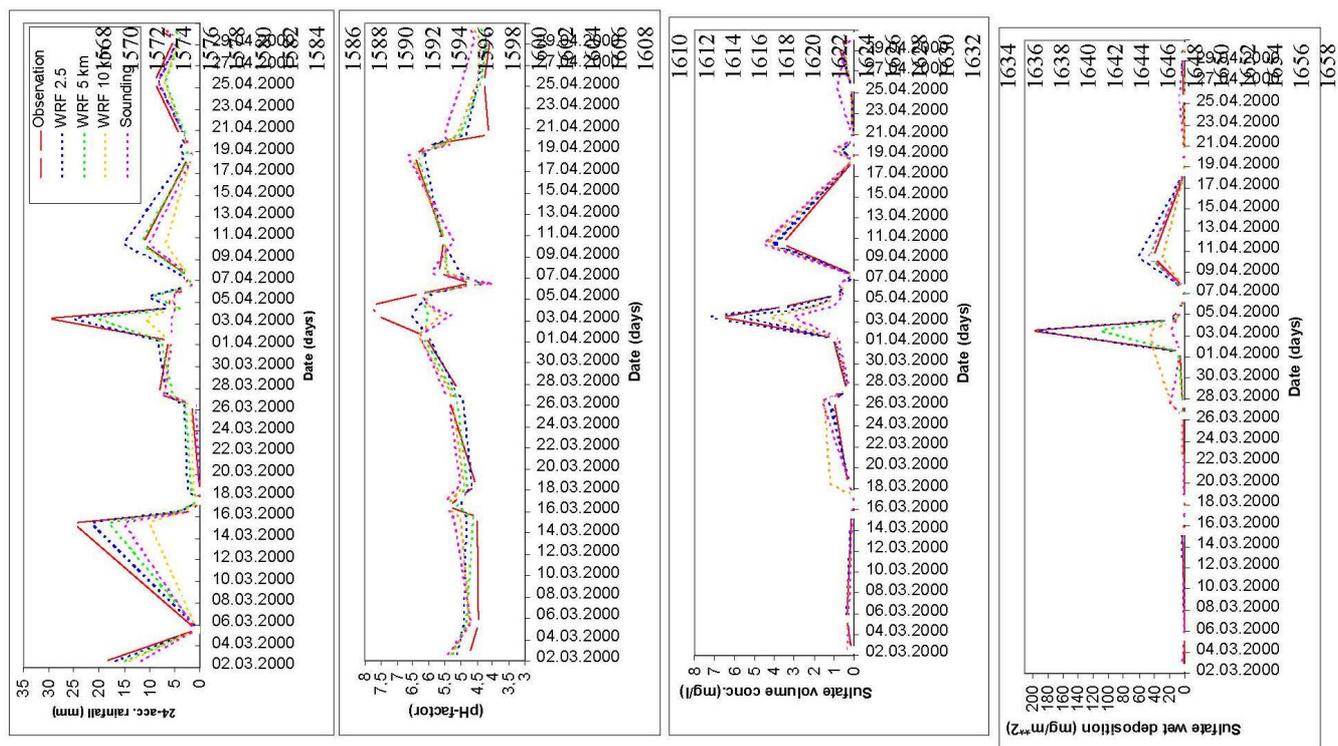
Figure 13: (a) Volume concentration of SO_4^{2-} (mg/l), (b) wet deposition of SO_4^{2-} as Sulphur (mg/m^2) and (c) pH value found in precipitation, in period March-April 2000.

5. Conclusions

A cloud model coupled with sulfate chemistry sub-model has been used to examine the sulfate production and wet deposition over a rural location in Macedonia during March-April 2000. A set of numerical experiments has been performed with WRF model conditions, using different horizontal grid resolution. Our main motivation is to evaluate the model ability and its performance in simulation of aqueous phase sulfate chemistry in convective cloud. The cloud-chemistry model is initialized with an ellipsoidal thermal bubble with minimal temperature perturbation of 0.2 in the bubble center. The chemical field initialization is based on the vertical distribution profile of chemical species participating in sulfate chemistry provided from the laboratory measurements at Lazaropole station using standard chemical analysis of rainfall samples, carried our within EMEP Program. The analysis shows that the maximum volume concentration of SO_4^{2-}, pH value and wet deposition is measured on 3 April 2000 when considerable dust was transported into atmosphere. Numerical simulation with initialization derived from WRF 2.5 km forecast and explicit treatment of convection provides a more realistic simulation of the structural and evolution properties of cloud with chemistry during the whole life cycle of cloud and better represents the cloud chemistry interactions and the modification of the pollutant concentration. It is evident that simulated sulfate concentration averaged over simulation time is very close to measured volume concentration compared to other runs, which use upper air sounding data as meteorological input and WRF forecast with 10 grid increment and cumulus parameterization. The study also includes the examination of the relative importance of scavenging, oxidation and ice-phase processes to sulfate production and wet deposition. Most of the sulfate aerosol production occurs in cloud developing phase when in-cloud oxidation of SO_2 by H_2O_2 and O_3 takes place. The sensitivity tests revealed that scavenging and oxidation contribute for about 33 and 46 % in sulphur production, while ignoring the ice-phase chemistry leads to 463 overprediction of sulfate for about 8% relative to the base run using WRF 2.5 km initialization. The comparative analysis has shown a relatively good agreement between simulated and measured data during the entire analyzed period with exception to total accumulated rainfall and the amount of wet deposition which in our study refers to 120 min simulation. The differences are more apparent when upper air sounding and coarser WRF forecast is used to initialize the cloud-chemistry model runs. As summary, the model sensitivity experiments which utilize this novel method of initialization derived from WRF model conditions with fine horizontal grid resolution, provides better representation of the local meteorological environment as important ingredient for cloud initiation and simulation of the convective scale processes which are responsible for cloud evolution, cloud chemistry interactions and transformation, sulfate production and subsequent deposition.

References

[1] Hales, J. M.1982: Mechanistic analysis of precipitation scavenging using a one-dimensional time variant model. Atmos. Environ., 16, 177-1783.

[2] Walcek, C. J. and Taylor, G. R.: A theoretical method for computing vertical distributions of acidity and sulfate production within cumulus clouds, J. Atmos. Sci, 43(4), 339-355, 1986.

[3] Taylor, G. R.: Sulfate production and deposition in mid-latitude continental cumulus clouds II, Chemistry model formulation and sensitivity analysis. J.Atmos. Sci., 46(13), 1991-2007, 1989.

[4] Tremblay, A. and Leighton, H.: A three-dimensional cloud chemistry 592 model. J. Climate Appl.Meteor., 25, 652-671, 1986.

[5] Niewiadomski, M.: Sulfur dioxide and sulfate in a three-dimensional field of convective clouds: Numerical simulations, Atmos. Environ., 23(2), 477-487, 1989.

[6] Wang, C. and Chang, J. S.: A three-dimensional numerical model of cloud dynamics, microphysics and chemistry, 4. Cloud chemistry and precipitation chemistry, J. Geophys. Res., 98, 116,799-16,808, 1993a.

[7] Wang, C. and Chang, J. S.: A three-dimensional numerical model of cloud dynamics, microphysics, and chemistry, 1.Concepts and formulation, J.Geophys.Res.,98, 14,827-17,844, 1993b.

[8] Wang, C. and Crutzen, P. J.: Impact of a simulated severe local storm on the redistribution of sulfur dioxide, J. Geophys. Res., 100, D6, 11357-11367, 1995.

[9] Kreidenweis, S. M., Zhang, Y., and Taylor, G. R.: The effects of clouds on aerosol and chemical species production and distribution, 2. Chemistry model description and sensitivity analysis, J. Geophys. Res., 102, 23,867-23,882, 1997.

[10] Wang, C. and Prinn, R. G.: Impact of the horizontal wind profile on the convective transport of chemical species. J. Geophys. Res., 103, D17, 22063-22071, 1998.

[11] Wang, C. and Prinn, R. G.: On the roles of deep convective clouds in tropospheric chemistry. J. Geophys. Res., 105, 22,269-22,297, 2000.

[12] Spiridonov, V. and Curic, M.: A three-dimensional numerical simulation of sulfate transport and redistribution. Can. J. Phys. 81: 1067-1094, 2003.

[13] Spiridonov, V. and Curic, M.: The relative importance of scavenging, oxidation and ice-phase processes in production and wet deposition of sulfate. J.Atmos.Sci. 2118-2135, 62, 2005.

[14] Spiridonov, V. and Curic, M.: Numerical simulation of physical and chemical processes in convective clouds. Asia-Pacific Journal of Atmospheric Sciences, 45, 1, 2009.

[15] Barth, M. C., Stuart, A. L., and Skamarock, W.C.: Numerical simulations of the July 10 STERAO/Deep Convection storm: Redistribution of soluble tracers, J. Geophys. Res., 106, 12 381–12 400, 2001.

[16] Yin, Y., Parker, D. J., and Carslaw, K. S.: Simulation of trace gas redistribution by convective clouds-Liquid phase processes. Atmos. Chem. Phys., 1, 19-36, 2001.

[17] Ekman, A. M., Wang, C, Wilson, J., and Strom, J.:2004 Explicit simulation of aerosol physics in a cloud resolving model. Atmos. Chem. Phys. Discuss., 4, 753-803.

[18] Ekman, A. M., Wang, Strom, J., and Krejci, R., 2006:Explicit Simulation of Aerosol Physics in a Cloud-Resolving Model: Aerosol Transport and Processing in the Free Troposphere. J.Atmos. Sci. 63,693-696, 2006.

[19] Stuart, A. L. and Jacobson, M. Z.: A timescale investigation of volatile chemical retention during hydrometeor freezing: Nonrime freezing and dry growth riming without spreading. J. Geophys. Res., 108(D6), 4178, 2003.

[20] Barth, M. C., et al.: Simulations of the redistribution of formaldehyde, formic acid, and peroxides in the 10 July 1996 Stratospheric-Tropospheric Experiment: Radiation, Aerosols, and Ozone deep convection storm, J. Geophys. Res. Vol. 112, D13310, doi:10.1029/2006JD008046, 2007a.

[21] Wonaschuetz, A, Sorooshian, A, Ervens, B, Chuang, P.Y., Feingold, G., Murphy, S, Gouw, J. de Warneke, C., and Jonsson, H.H., Aerosol and Gas Re-Distribution by Shallow Cumulus Clouds: An Investigation Using Airborne Measurements." Journal of Geophysical Research: Atmospheres 117.D17202, 1-18, 2012.

[22] Vujović, D, Vučković, V, and Ćurić, M.: Effect of topography on sulfate redistribution in cumulonimbus cloud development, Environ Sci. Pollut. Res., 21:3415–3426, 2014.

[23] Berg L. K., Shrivastava1, N. Easter, R.C. , Fast, J.D. Chapman, E.G., Liu, Y. and Ferrare, R.A.: A new WRF-Chem treatment for studying regional-scale impacts of cloud processes on aerosol and trace gases in parameterized cumuli, Geosci. Model Dev., 8, 409–429, 2015.

[24] Barth, M. C., et al.: The Deep Convective Clouds and Chemistry (DC3) field campaign, Bull. Am. Meteorol. Soc., 96(8), 1281–1309, doi:10.1175/BAMS-D-13-00290.1, 2015.

[25] Barth, M. C., et al. (2016), Convective transport of peroxides by thunderstorms observed over the Central U.S. during DC3, J. Geophys. Res. Atmos., doi:10.1002/2015JD024570.

[26] Bela, M. M., et al. (2016), Wet scavenging of soluble gases in DC3 deep convective storms using WRF-Chem simulations and aircraft observations, J. Geophys. Res. Atmos., 121, 4233–4257, doi:10.1002/2015JD024623.

[27] Klemp, J. B. and Wilhelmson, R. B.: The simulation of three-dimensional convective storm dynamics. J. Atmos. Sci., 35, 1070-1096, 1978.

[28] Orville, H. D. and Kopp, F. J.: Numerical simulation of the history of a hailstorm. J. Atmos. Sci., 34, 1596-1618, 1977.

[29] Lin, Y.L., Farley, R. D., and Orville, H. D.: Bulk water parameterization in a cloud model. J. Climate Appl. Meteor., 22, 1065-1092, 1983.

[30] Telenta, B. and Aleksic, N.: A three-dimensional simulation of the 17 June 1978 HIPLEX case with observed ice multiplication. 2nd International Cloud Modeling Workshop, Toulouse, 8-12 August 1988. WMO/TD No. 268, 277-285, 1988.

[31] Barth et al: Cloud-scale model intercomparison of chemical constituent transport in deep convection, Atmos. Chem. Phys., 7, 4709-4731, 2007b.

[32] Janjic, Z.I., 2001: Nonsingular implementation of the Mellor-Yamada level 2.5 scheme in the NCEP Meso model. NOAA/NWS/ NCEP Office Note 437, 61 pp

[33] Janjic, Z. I., 2003a: A Nonhydrostatic Model Based on a New Approach. Meteorology and Atmospheric Physics, 82, 271–285.

[34] Janjic, Z. I., 2003b: The NCEP WRF Core and Further Development of Its Physical Package. 5th International SRNWP Workshop on Non-Hydrostatic Modeling, Bad Orb, Germany, 27-29 October.

[35] Janjic, Z. I., 1990: The step-mountain coordinate: Physical package. Mon. Wea. Rev., 118, 1429–1443.

[36] Janjic, Z.I, 1994: The Step-Mountain Eta Coordinate Model: Further developments of the convection, viscous sublayer, and turbulence closure schemes. Mon. Wea. Rev., 122, 927–945.

[37] Chen, F. and J. Dudhia, 2001: Coupling an Advanced Land Surface-Hydrology Model with the Penn State-NCAR MM5 Modelling System. Part I: Model Implementation and Sensitivity. Mon. Wea. Rev., 129, 569-585.

[38] Hong, S.Y. and J.J.Lim, 2006: The WRF Single-Moment 6-Class Microphysics 543 Scheme (WSM6), Journal of the Korean Meteorological Society, 42, 2, p. 129-151.

[39] Giorgi, F., and W. L. Chameides: Rainout lifetimes of highly soluble aerosols and gases as inferred from simulations with a general circulation model. J. Geophys. Res., 91, 14367–14376, 1986.

[40] Easter, R. C., and J. M. Hales: Interpretation of the OSCAR data for reactive gas scavenging. Precipitation Scavenging, Dry Deposition, and Resuspension, H. R. Pruppacher, R. G. Semonin, and W. G. Slinn, Eds., Elsevier, 649–662, 1983.

[41] Cohan, D. S., M. G. Schultz, D. J. Jacob, B. G. Heikes, and D. R. Blake,: Convective injection and photochemical decay of peroxides in the tropical upper troposphere: Methyl iodide as a tracer of marine convection. J. Geophys. Res., 104, 5717–5724, 1999.

[42] Crutzen, P. J., and M. G. Lawrence: The impact of precipitation scavenging on the transport of trace gases: A 3-dimensional model sensitivity study. J. Atmos. Chem., 37, 81–112, 2000.

[43] Bae, S.Y., Park, R.J., Kim, Y.P., Woo, J.-H., 2012. Effects of below-cloud scavenging on the regional aerosol budget in East Asia. Atmos. Environ. 58, 14–22.